RESEARCH PAPER

ZnO Biological Nanomaterials: Synthesis and Morphological Analyses for Applications in Worthwhile Electrochemical Devices in Medical Field

M. Maheswari[1], K. Neyvasagam[2]

[1]Principal, Department of Physics, Noble College of Arts and Science for Women, Aruppukottai-Virudhunagar Main Road (SH42), Palavanatham-626004. maheshsubramaniankk@gmail.com
[2]Associate Professor, PG and Research Department of Physics, The Madura College, Madurai-625011. srineyvas@yahoo.co.in

Abstract
Because of their special qualities and the fact that they include a broad variety of samples with at least one dimension between 1 and 100 nm, nanomaterials have drawn a lot of attention as an amazing class of materials. Nanomaterials have been a major focus of study in the development of affordable electrochemical devices for energy storage and conversion applications. Due to its remarkable characteristics, numerous studies have been conducted with the goal of enhancing the efficiency and affordability of electrochemical devices, such as fuel cells, batteries, and supercapacitors. The electrochemical performance of electrodes, energy storage, and nanotechnology-based electrochemical sensors (ES) are the main topics of this paper. Additionally, it examines the difficulties faced by enterprises based on nanotechnology as well as the integration of nanostructures with electrochemical systems in commercially significant and future applications. The interaction between nanomaterials and biosensors—which are essential components of electrochemical devices—is also examined in this research. The several biological processes for producing nanostructured materials were examined in this article, along with their characteristics and methods of characterization. Because of their sustainability, affordability, speed, non-pathogenic nature, environmental friendliness, ease of scaling up for large-scale synthesis, and lack of requirement for high pressure, temperature, or hazardous chemical components, biological approaches are becoming more and more popular in the synthesis of nanomaterials. They are also used safely and effectively for human therapeutic purposes. Additionally, a variety of methods, including energy-dispersive X-ray spectroscopy, Transmission electron microscopy (TEM), are used to characterize the surface morphology and compositional structure of nanomaterials.

Keywords: Biological Nanomaterials; Nanotechnology; Compositional Structure; Electrochemical Devices; Worthwhile; Storage Devices
How to cite this article: Maheswari M, Neyvasagam K., ZnO Biological Nanomaterials: Synthesis and Morphological Analyses for Applications in Worthwhile Electrochemical Devices in Medical Field. Int J Drug Deliv Technol. 2026;16(77s): 1299-1308; DOI: 10.25258/ijddt.16.77s.151

Literature Survey

The development of cost-effective electrochemical devices is crucial for efficient energy storage and conversion, which is essential for sustainable development. Nanomaterials have demonstrated great potential in enhancing the performance of electrochemical devices, but the synthesis of these materials for large-scale applications remains a challenge [1]. Several synthesis methods have been developed to address this challenge, including solutionbased, template-based, and microwave-assisted synthesis. These methods have shown promise in producing high-quality nanomaterials in large quantities, and they have the potential to reduce production costs. Integrating nanomaterials into electrochemical devices is also a significant challenge, as the properties of nanomaterials differ significantly from those of their bulk counterparts [2]. The interface between the nanomaterials and other components of the electrochemical device is critical, and it can significantly influence device performance and efficiency. Therefore, optimizing the integration of nanomaterials into electrochemical devices is crucial for realizing their full potential.

The synthesis of nanomaterials on a large scale for practical applications remains a challenge. However, significant progress has been made in developing various synthesis methods, such as solution-based methods, template-based methods, and microwave-assisted synthesis [3, 4]. These approaches show promise in producing high-quality nanomaterials in large quantities while also potentially reducing production costs.

Integrating nanomaterials into electrochemical devices presents another significant challenge. The properties of nanomaterials differ significantly from their bulk counterparts, necessitating careful consideration of their integration with other components of the device. The interface between nanomaterials and the device's other constituents critically influences device performance and efficiency [5]. Therefore, optimizing the integration of nanomaterials is crucial to fully exploit their potential in electrochemical devices [5]. One key aspect that distinguishes nanomaterials in electrochemical applications is their electrical properties. Nanomaterials can be broadly classified as conductive, semiconductive, or insulating based on their ability to conduct electricity. Conductive nanomaterials, such as carbon nanotubes and graphene, exhibit high electrical conductivity and find extensive use as current collectors, electrodes, and

catalysts. Semi-conductive nanomaterials, such as metal oxides and sulfides, possess moderate electrical conductivity and can serve as active materials for energy storage and conversion.

Insulating nanomaterials, including metal–organic frameworks (MOFs) and covalent organic frameworks (COFs), offer low electrical conductivity but provide high surface area and large pore volumes, making them suitable support materials for electrochemical devices [6].

Moreover, the composition of nanomaterials also affects their electrical properties. Innovative nanomaterials like MOFs, COFs, and MXenes have gained considerable attention due to their tunable electrical properties and high surface areas, making them promising candidates for electrochemical device applications [6].

Table 1 Nanomaterials Applied to Different Electrochemical Equipment

Electrochemical Device	Nanomaterials Used	Applications	Ref.
Batteries	Nanostructured metals, metal oxides, and carbon-based materials, MOFs, COFs, MXenes.	Electrode materials to boost energy and power densities, enhance performance, expand surface area, and improve conductivity	10
Supercapacitors	Carbon nanotubes, graphene, and other carbon-based materials, MOFs, COFs, and MXenes.	Electrode materials that offer high power and energy densities, enhance conductivity, and expand surface area	11, 12
Fuel Cells	Platinum, gold, and other metal nanoparticles, MOFs, COFs, MXenes.	Catalysts that increase the effectiveness of electrochemical processes that produce power	13
Sensors	Metal nanoparticles, metal oxides, and carbon-based materials, MOFs, COFs, MXenes	Because of their large surface area, strong catalytic activity, and distinct optical and electrical characteristics, sensing elements can increase sensitivity and selectivity.	14

Overall, the unique properties of nanomaterials make them attractive for use in electrochemical devices, and their potential for cost-effectiveness makes them even more appealing. By understanding the different types of nanomaterials and their properties, researchers can continue to develop new and improved electrochemical devices with enhanced performance and cost-effectiveness. Therefore, this review will highlight electrochemical techniques, energy storage, as well as electrochemical sensors based on nanotechnology. As well as the integration of nanostructures with the electrochemical system in applications of economic interest. It will shed light on the future of these applications and the challenges of environmental sustainability.

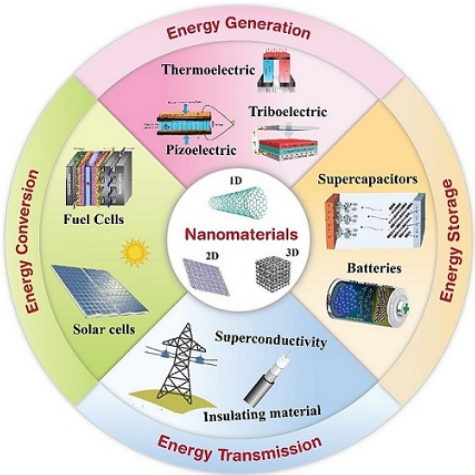

Scheme 1 and Table 1 Summarize the Use of Nanomaterials Applied to Different Electrochemical Equipment

Moreover, innovative sustainable materials have been used in nuclear applications such as cellulosic waste in treatment [7, 8] or cement mixed with plant waste [9], natural clay [10], bitumen [4] or with asphaltene and polymer [6], cement waste [7], and glass [8-10] for waste stabilization and radiation shielding.

Nanomaterials can be categorised as 0D, 1D, and 2D structures according to their dimensions. The most basic kind of nanomaterials are spherical nanoparticles known as zero-dimensional (0D) nanomaterials. Metal nanoparticles like gold and silver, semiconductor nanoparticles like quantumdots, and oxide nanoparticles like titanium dioxide are a few examples of 0D nanomaterials [15]. The electric characteristics of nanomaterials, such as their insulating,

semiconducting, and metal-like qualities, can also be used to categorise them. Insulating nanomaterials have a large band gap and don't carry electricity.
Metal oxides such as titanium dioxide, zinc oxide, and aluminium oxide are examples of insulating nanomaterials. Catalysis, energy storage, and environmental cleanup are just a few of the numerous uses for these nanomaterials.
A categorization based on various material classes has been developed to better comprehend and classify the many kinds of nanomaterials that can be employed in electrochemical applications. These categories include conducting polymers, metal oxides and hydroxides, carbon-based nanomaterials, and hybrid materials. The performance of electrochemical devices, especially in energy storage applications like batteries and supercapacitors, can be greatly enhanced by carbon-based nanomaterials like graphene, carbon nanotubes, and fullerenes, which have been thoroughly investigated [16].

Applications of Nanomaterials in Electrochemical Devices

Because of their high surface area and redox characteristics, metal hydroxides and oxides, such as iron oxide, zinc oxide, and titanium dioxide, has also showed promise in electrochemical devices [17]. A variety of electrochemical applications can benefit from the special qualities of conducting polymers like polyaniline and polypyrrole, which include high conductivity and adjustable redox potential. Research has also been done on hybrid materials, which combine two or more kinds of nanomaterials and have the potential to improve functionality and performance. The electro-chemical properties of the devices are significantly changed when electroactive materials are nanostructured. Two- and three-dimensional nanometer-sized structures, such as dye-sensitized solar cells (DSSC), are assembled from quasi-zero-dimensional structures or building blocks (nanoparticles). Furthermore, because of their tiny size and large surface area, 0D nanoparticles and nanodots have garnered a lot of interest for their possible application in batteries. Specifically, 0D nanoparticles and nanodots have special chemical and physical characteristics that make them attractive options for battery electrode materials.
By offering high capacity, quick charging and discharging rates, and an extended cycle life, these materials can greatly enhance battery performance [18].
The large surface area of 0D nanoparticles and nanodots, which offers many active sites for electrochemical reactions, is one of its advantages. Because more active material is accessible for electrochemical processes, this characteristic can increase battery capacity [19]. Furthermore, quick diffusion of lithium ions is made possible by the tiny size of 0D nanoparticles and nanodots, which results in quicker charging and discharging rates. Because of their large surface area-to-volume ratio, 0D nanoparticles and nanodots have two advantages when used in batteries: improved electrochemical performance and more effective ion transport [19].
Numerous kinds of 0D nanoparticles and nanodots, such as metal oxide nanoparticles, carbon nanodots, and quantum dots, have been studied. For example, research has demonstrated that carbon nanodots may increase the capacity and rate performance of sodium-ion batteries, while tin oxide nanoparticles can improve the cycle stability and rate capability of lithium-ion batteries [20]. Due to their special electrical and optical characteristics, quantum dots have also been studied for their application in next-generation batteries [20].
Furthermore, the special qualities of 0D nanoparticles and nanodots make them appealing for application in a variety of electrochemical devices other than batteries. For example, they are perfect for usage in sensors, catalysts, and supercapacitors due to their high surface area-to-volume ratio and adjustable size and shape. Their compact size can also improve ion diffusion and electron transport, which will improve the overall performance of the device.
The development of new synthetic techniques for creating extremely homogeneous and monodisperse 0D nanoparticles and nanodots, as well as investigating their electrochemical characteristics and possible uses in a range of electrochemical devices, have been the main focus of recent research [21]. 1D nanowires and 2D nanosheets have been extensively studied for use in a variety of electrochemical devices, including fuel cells and supercapacitors [22]. Because of their enormous surface area and superior conductivity, these materials show high specific capacitance and quick charge/discharge rates in supercapacitors. 1D nanowires and 2D nanosheets have been employed as catalysts in fuel cells to enhance reaction kinetics and lower electrochemical reaction costs. 1D and 2D nanomaterials are appealing for a variety of electrochemical device applications due to their special qualities, such as their mechanical strength, flexibility, and transparency [23].
The potential application of three-dimensional (3D) nanometer-sized structures, also referred to as nanoarchitectures or nanostructures, in electrochemical devices has also been studied. The performance of electrochemical devices and electrochemical processes can be improved by these structures' high surface area and distinctive porosity [24]. Mesoporous silica, nanocubes, and nanorods are examples of three-dimensional nanostructures. With encouraging outcomes, researchers have investigated their application in fuel cells, batteries, and supercapacitors. To fully realise the promise of these materials, additional research is required to overcome the remaining obstacles in the synthesis and integration of 3D nanostructures into useful electrochemical devices.
For the identification and characterisation of nanoparticles, specific analytical methods are employed. Electron microscopes for scanning or transmission (SEM, TEM) are examples of advanced technology [22–24]. Different optical techniques can yield different kinds of physicochemical information on nanoparticles, but the technology and specific material attributes, such composition and size, determine how relevant they are. Certain issues, such inexpensive, user-friendly portable controllers and self-powered gadgets, can be resolved using electrochemical technology.

Nanotechnology may be a potential option for many electrochemical technologies since many nanoparticles can produce electrical signals, have good biocompatibility and stability, and are easy to use [25].

To assist the development and execution of biomonitoring programs, quantitative methods are needed to measure exposure to alien organisms. Chemical synthesis, electroextraction, metal refinement, batteries, fuel cells, sensors, and surface modification thru electrostatic precipitation, separation, and corrosion are just a few of the numerous technical uses for the electrochemical phenomena. The significance of nanotechnology in developing suitable electrode materials for high-performance supercapacitors has been highlighted by recent research [26].

Zheng et al.'s [27] discovery of a template-free, one-step carbonization-activation method significantly simplified the synthesis of nitrogen-rich activated nanosized carbon with hierarchical micro/mesoporous and ultrahigh specific surface area while reducing chemical waste. Using a mechanically driven sol–gel transition technique, chitin nanoparticles were synthesised in a NaOH/urea solvent to produce activated carbon with a high nitrogen content and robust electrochemical properties. We compare the different kinds of nanomaterials utilised in different electrochemical devices in T**able 2.**

Table 2 A comparative study of the morphological characteristics and properties of nanomaterials produced using various techniques

Nanomaterials	Synthesis Method	Morphological Features	Properties	Ref.
Metal oxides and hydroxides	Various synthesis methods	High surface area, redox properties	Suitable for electrochemical devices	28, 29
Conducting polymers (e.g., polyaniline, polypyrrole)	Various synthesis methods	High conductivity, tunable redox potential	Versatile for electrochemical applications	30
Hybrid materials	Mixing different kinds of nanomaterials	Enhanced functionality and performance	Enhanced properties through synergy	31, 32
0D nanoparticles and nanodots	Various synthesis methods	Small size, high surface area	Promising for batteries, sensors, catalysts, Supercapacitors	33
1D nanowires and 2D nanosheets	Various synthesis methods	Large surface area, excellent conductivity	Ideal for supercapacitors, fuel cells, and other electrochemical devices	35
3D nanostructures (nanocubes, nanorods, mesoporous silica)	Various synthesis methods	High surface area, unique porosity	Potential for batteries, supercapacitors, fuel cells	35, 36
Nanomaterials for electrode materials	Various synthesis methods	Tailored properties for high-performance device	Potential for electrochemical devices	36

Because of their large surface area and redox characteristics, metal oxides and hydroxides including iron oxide, zinc oxide, and titanium dioxide are appropriate for electrochemical applications. Because of their high conductivity and adjustable redox potential, conducting polymers like polyaniline and polypyrrole offer flexibility in electrochemical devices. Because of their synergistic effects, hybrid materials—which blend several nanomaterial classes—offer enhanced functionality and performance. Additionally, nanomaterials with specific characteristics for high-performance devices are created for electrode materials in electrochemical devices. Researchers can create more affordable electrochemical devices with improved performance by comprehending the unique properties and production techniques of these nanomaterials.

Materials Used

Zinc acetate dihydrate (Zn(CH3COO)2·2H2O) from Sigma-Aldrich Chemical Company (St. Louis, MO, USA), deionised water containing 1 M ammonium hydroxide (30% of the concentration in the container), ethylene glycol (solvent 99.8%), and isopropyl alcohol (solvent 99.9%).

Synthesis ZnO Nanomaterials using Hydrothermal Route

The hydrothermal method was used to create the ZnO nanomaterials [37]. Because of its low cost and low temperature, the hydrothermal approach is one of the most used synthesis techniques for the creation of ZnO nanorods.

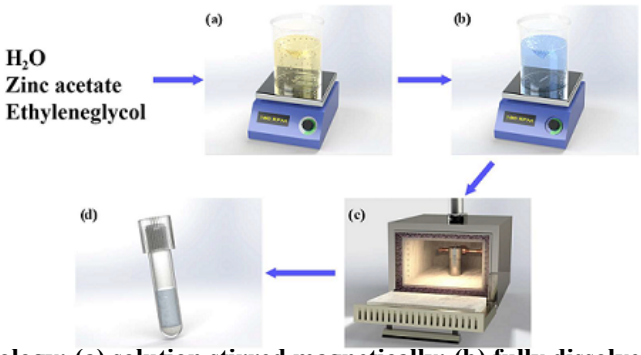

Figure 1 Reaction methodology: (a) solution stirred magnetically; (b) fully dissolved solution; (c) solution placed in a Teflon-lined stainless steel autoclave in a muffle; and (d) solution cleaned and centrifuged.

The reactions were put in a beaker and stirred magnetically until all of the ingredients were fully dissolved (Figure 1a and b). For each reaction, 500 mg of zinc acetate dihydrate were dissolved in 10 mL of ethylene glycol and 3 mL of deionised water. 50 microlitres of deionised water containing 1 M ammonium hydroxide were used for reactions with (*). To fully dissolve the zinc acetate, this liquid was magnetically agitated for 20 hours. The solutions were then placed in a stainless steel autoclave lined with Teflon and allowed to react (Figure 1c).

Table 3 Temperature and duration of each reaction

Reaction	Temperature (◦C)	Time (Min)
ZnO-1	160	89
*ZnO-1	150	95
ZnO-2	140	183
*ZnO-2	150	183
ZnO-3	150	359

Ammonium hydroxide was utilised in processes using (*).

The temperature and duration of each reaction are displayed in Table 3. After three centrifugations at 15,000 rpm for 15 minutes, the products were cleaned with isopropyl alcohol (Figure 1d). Zinc acetate may be dissociated by the heat and high pressure created in the reactor by ethylene glycol, producing Zn2+ ions. The acetate ions then react with the water to make hydroxyl ions and acetic acid. Zinc hydroxide, which can produce oversaturated nucleation sites and precipitate in more stable species for temperature and reaction time, can be produced when the hydroxyl ions bond to Zn2+. ZnO nucleates in a heterogeneous environment when the Zn(OH) dehydrates.
More hydroxyl ions may be produced by ammonium hydroxide, which favours Zn(OH) and shortens the ZnO growth period.

$$2Z(CH_3COO)_2 \cdot 2H_2O \rightarrow 2Zn^{2+} + 4(CH_3COO)^- + 4H_2O_2$$

$$2Zn^{2+} + 4OH^- \rightarrow Zn_2(OH)_4$$

$$Zn_2(OH)_4 \rightarrow 2ZnO$$

Morphological Studies

Powder X-ray diffraction measurements were made with KαCu (λ = 1.54 Ao) using a Ni filter Ultima IV (Rigaku, Tokyo, Japan), operated in a Bragg– Brentano geometry with 40 kV voltage and 44 mA of emission current, equipped with a D/tex Ultra detector.
The diffraction patterns were registered in an angular interval from 20◦ to 80◦ at 2θ with an angular resolution of 0.02◦ and velocity of 10◦/min. The powder was put on a glass holder sample. The morphological study was realized by transmission electron microscopy with a TITAN microscope supplied by FEI-Company (Hillsboro, OR, USA). The samples were prepared with a few drops of ZnO redispersed in isopropyl alcohol (0.1 mg/mL) on a lacey carbon grid. Finally, the electrical behavior was characterized by the Precision PiezoMEMS tester for Radiant Technologies, Inc. (Albuquerque, NM, USA) equipment.

Outcomes and Implications with Data Analyses

1. X-ray diffractogram Analyses

ZnO Nanomaterials' X-ray diffractogram exhibits acceptable quality in all processes and reveals no precursor residue or impurities. The creation of a hexagonal wurtzite phase is demonstrated by reflections that align with the crystalline planes of the material structure (Figure 2). Additionally, the peak widening indicates that samples may include tiny nanocrystals.

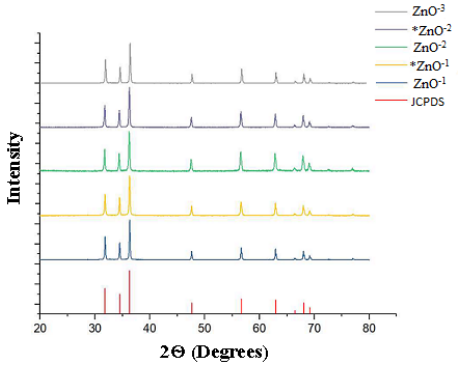

Figure 2 XRD traces for every reaction

The Scherrer equation was used to compute the mean crystallite size before determining the dislocation density. Additionally, wurtzite lattice constants and interplanar distance were measured and compared with the data reported under JCPDS Card No. 36–1451 (Tables 3a and 3b).

Consequently, the lattice constants were used to compute the bond length from the tetrahedral of the wurtzite structure, demonstrating the little or nonexistent presence of strain in the ZnO nanomaterials. Additionally, an effective mass model was used to compute the ZnO Nanomaterials' band gap [38, 39].

Calculation: Crystallite Size and Lattice Parameters

A crystallite is a region of a material that shares the same crystallographic orientation. The size of metallic, ceramic, and polymeric nanomaterials greatly affects their mechanical, chemical, and physical properties [40].

Using the Scherrer equation, we calculated the average crystallite size of each reaction (Tables 4a and 4b):

$$D = \frac{k\gamma}{\beta \cos\theta} \qquad (1)$$

where D is the size of the crystallites, k = 0.9 is the Scherrer constant, γ = 0.15 is the X-ray source's wavelength in nanometres, β is the Full Width at Half Maximum (FWHM) in radians, and θ is the peak location (in radians). Each plane's crystallite size was measured, and the average size, Dm, was found.

$$\delta = \frac{1}{D_m^2} \qquad (2)$$

The average crystallite size for each reaction was used to compute, which is defined as a line of structural discontinuities running thru each crystal or grain per unit of volume (Table 4). Significant peak broadening may result from the samples' extensive dislocations. Dislocation density and crystallite size are important components of diffraction analysis because of their consequences [41].

Table 4 Crystallite size (nm) for each plane, mean size (nm), and dislocation density ∂ (nm−2) for each ZnO Nanomaterials reaction

Plane <h,k,l>	ZnO-1	*ZnO-1	ZnO-2	*ZnO-2	ZnO-3
Dm	30.8	32.0	29.5	30.9	34.7
δ = 10 -4	10.5	9.7	11.4	10.4	8.3

Ammonium hydroxide was utilised in processes using (*).

Zinc and oxygen atoms are organized in a hexagonal closed pack, coordinating with one another in an equal location. Furthermore, Bragg's rule was used to compute the interplanar gaps from the wurtzite structure [41].

The Miller indices characterize each pair of crystallographic planes, and we computed the interplanar distance, which is a function of the unit cell parameters, to produce the lattice constants. Lattice constants a and c are related to the inverse square of the interplanar distance in a hexagonal crystal structure. In the end, a and c were computed using planes (1 0 0) for a and (0 0 2) for c. The (h k l) planes listed in the JCPDS card data match the interplanar distances determined by XRD. Additionally, Table 5 compares the lattice parameters computed for each response to the JCPDS card.

Table 5 Lattice parameters from XRD data and JCPDS data in Angstroms (A)

Lattice Parameters	ZnO-1	*ZnO-1	ZnO-2	*ZnO-2	ZnO-3	JCPDS
a	3.26	3.25	3.26	3.25	3.24	3.25
c	5.22	5.21	5.22	5.21	5.19	5.2
$\frac{c}{a}$	1.61	1.61	1.62	1.61	1.62	1.60
V	47.9	47.6	47.6	47.9	47.78	47.62

Ammonium hydroxide was utilised in processes using (*).

2. Transmission Electron Microscopy

Table 6 The ZnO nanomaterials' mean, standard deviation, minimum and maximum sizes (nm).

Reaction	Mean	Standard Deviation	Minimum	Maximum
Length (nm)				
ZnO-1	164	82	40	389
*ZnO-1	177	77	44	572
ZnO-2	150	81	43	558
*ZnO-2	341	139	67	952
ZnO-3	168	64	49	363
Width (nm)				
ZnO-1	72	24	33	145
*ZnO-1	87	32	31	256
ZnO-2	84	36	42	261
*ZnO-2	120	53	44	321
ZnO-3	83	28	43	209

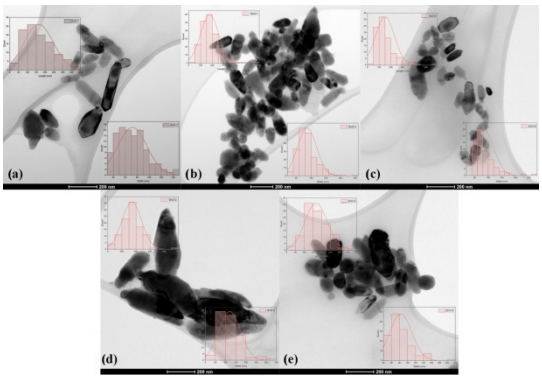

Figure 3 TEM pictures and histograms of each ZnO nanomaterial's length and breadth response: (a) ZnO-1, (b) *ZnO-1, (c) ZnO-2, (d) *ZnO-2, (e) ZnO-3 [Ammonium hydroxide was utilised in processes using (*)]

Particle production at the nanoscale is confirmed by the TEM pictures (Figure 3a–e), which display the breadth and broad histograms of each reaction's size distribution.

The length and breadth of these nanomaterials were measured and verified using the free program ImageJ (https://imagej.net/ij/). The ZnO nanomaterials' average length and breadth are between 150 and 341 nm and 72 and 120 nm, respectively. ZnO Nanomaterials of reaction ZnO-1, which have a distinct column form between length and breadth, are shown in Figure 3a. Figure 3b shows that ZnO Nanomaterials with a slightly pointed form and a high average size in both length and breadth were produced by the reaction *ZnO-1. However, Figure 3c demonstrates that the ZnO-2 reaction resulted in ZnO Nanomaterials with a crisp shape, and the distinction between length and breadth is still clearly visible. We find that reaction *ZnO-2 produced ZnO Nanomaterials with a crisper shape based on Figure 3d. Lastly, Figure 3e shows that ZnO Nanomaterials with a distinct shape between length and breadth were formed by reaction ZnO-3.

The morphology shows a sharpy form at the end of each nanomaterial, which might be caused by hydroxyl ion enrichment, and larger expansion upon interactions with ammonium hydroxide. More faces are therefore encouraged to grow. Conversely, reaction *ZnO-2 shows that a solution richer in hydroxyl ions yields particles with a more scattered size the longer the reaction period.

ZnO Nanomaterials' Application

The MTI-2100 fotonic sensor is a fiber-optic measurement system (with a dual channel) that performs noncontact displacement and vibration measurements. By using fiberoptic technology, MTI-2100 does not apply load on the measurement target, and it is not affected by magnetic and electrical fields. We used this MTI-2100 fotonic sensor to

measure the displacements of a beam that was fabricated using a steel substrate and a ZnO nanomaterials synthetized with our method. This was deposited on the outer surface of the steel substrate. A 20 MHz DDS function generator (BK PRECISION 4040B) and a digital oscilloscope (Agilent Technologies DSO3102A, Santa Clara, CA, USA) were used in the measurements of the displacements of the beam, which were generated by the supplied voltages.

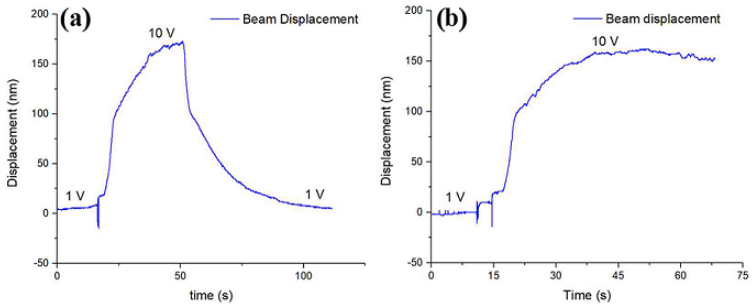

Figure 4 Displacement of a beam made of a ZnO nanomaterials produced by 1 Hz square wave voltages. Voltages from (a) 1 to 10 and 1 V and (b) 1 to 10 V were supplied.

Square wave voltages from 1 to 10 V with a frequency of 1 Hz were supplied to the beam, which generated displacements of the beam (Figure 4 a,b). The beam displacement was generated by the ZnO piezoelectric materials. A second measurement of the beam was made with square wave voltages at 50 Hz and values from 1 to 10 V and 10 to 1 V (see Figure 5 a,b). These measurements showed the piezoelectric effect of the ZnO Nanomaterials that was deposited on the beam surface.

When the supplied voltage is kept constant, the displacement of the beam is also kept constant. For voltages of 10 V at 1 and 50 Hz, the maximum displacement of the beam was close to 150 nm.

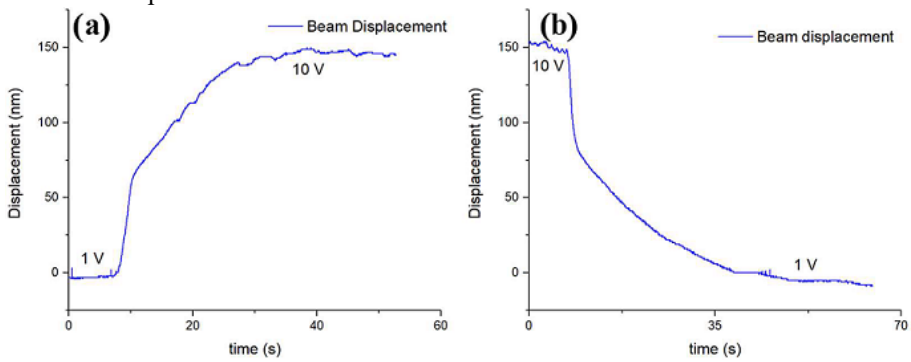

Figure 5 Displacement of a beam made of a ZnO Nanomaterials produced by 1 Hz square wave voltages. Voltages from (a) 10 to 1 and 1 V and (b) 10 to 1 V were supplied.

Conclusions

The substantial influence of nanomaterials on the future of several sectors and scientific fields is highlighted by the conclusion derived from the thorough study and findings reported in this publication. The necessity for ongoing developments in the field of nanotechnology is highlighted by the requirement for innovative technologies that can manipulate materials at the nanoscale. Because of their special qualities—such as their vast surface areas, distinct architectures, and abundance of active sites—nanomaterials have shown to be incredibly useful in improving electrochemical performance. This quest for increased cost-effectiveness and efficiency creates new opportunities for the commercialisation and broad use of nanomaterial-based solutions. Nanomaterials seem to have a very bright future.

Using a hydrothermal technique, we investigated the effects of reaction time and ammonium hydroxide addition on the form and characteristics of ZnO nanomaterials. Reactions without ammonium hydroxide produced the finest morphological control of the ZnO nanomaterials, most likely as a result of increased development along certain crystal faces. With the exception of reaction *ZnO-2, which displayed a bathochromic shift that can be linked to easy nucleation under changed circumstances, optical examination revealed a blue shift in comparison to bulk ZnO in the majority of samples.

Regardless of the presence of hydroxide, XRD measurements verified high crystallinity and consistent crystallite sizes throughout processes, and computed band gaps closely matched values found in the literature, supporting the validity of

the suggested synthesis. However, more characterisations are needed to optimise the suggested synthesis since the size and shape of the ZnO nanomaterials affect their mechanical and electrical characteristics. Additionally, a ZnO nanomaterials was applied to a steel beam's surface in order to evaluate the displacements caused by the piezoelectric effect at square wave voltages of 1 and 10 V at 1 and 50 Hz. These ZnO nanomaterials may be utilised to create nanotransducers, self-powered sensors, biosensors and piezoelectric nanogenerators.
More chemical analyses of the ZnO nanomaterials will be examined in further studies.
Funding: There was no external funding agency support for this research.
Conflicts of Interest: No conflicts of interest are disclosed by the authors.

Bibliographic References:

1. Dimensional Nanomaterials. In Nanomaterials Synthesis; Elsevier: Amsterdam, The Netherlands, 2019; pp. 1–25.
2. Ouyang, D.; Huang, Z.; Choy, W.C.H. Solution-processed Metal Oxide Nanocrystals as Carrier Transport Layers in Organic and Perovskite Solar Cells. Adv. Funct. Mater. 2019, 29, 1804660.
3. Wang, Q.; Sun, J.; Wei, D. Two-Dimensional Metal-Organic Frameworks and Covalent Organic Frameworks. Chin. J. Chem. 2022, 40, 1359–1385.
4. Saleh, H.M.; Moussa, H.R.; El-Saied, F.A.; Dawod, M.; Bayoumi, T.A.; Abdel Wahed, R.S. Mechanical and Physicochemical Evaluation of Solidifed Dried Submerged Plants Subjected to Extreme Climatic Conditions to Achieve an Optimum Waste Containment. Prog. Nucl. Energy 2020, 122, 103285.
5. Bayoumi, T.A.; Saleh, H.M.; Eskander, S.B. Solidification of hot real radioactive liquid scintillator waste using cement–clay composite. Monatshefte Für Chem.-Chem. Mon. 2013, 144, 1751–1758.
6. Reda, S.M.; Saleh, H.M. Calculation of the Gamma Radiation Shielding Efficiency of Cement-Bitumen Portable Container Using MCNPX Code. Prog. Nucl. Energy 2021, 142, 104012.
7. Saleh, H.M.; Bondouk, I.I.; Salama, E.; Mahmoud, H.H.; Omar, K.; Esawii, H.A. Asphaltene or Polyvinylchloride Waste Blended with Cement to Produce a Sustainable Material Used in Nuclear Safety. Sustainabilitiy 2022, 14, 3525.
8. El-Sayed, A.M.; Faheim, A.A.; Salman, A.A.; Saleh, H.M. Sustainable Lightweight Concrete Made of Cement Kiln Dust and Liquefied Polystyrene Foam Improved with Other Waste Additives. Sustainability 2022, 14, 15313.
9. Eid, M.S.; Bondouk, I.I.; Saleh, H.M.; Omar, K.M.; Sayyed, M.I.; El-Khatib, A.M.; Elsafi, M. Implementation of Waste Silicate Glass into Composition of Ordinary Cement for Radiation Shielding Applications. Nucl. Eng. Technol. 2021, 54, 1456–1463.
10. Ehab, M.; Salama, E.; Ashour, A.; Attallah, M.; Saleh, H.M. Optical Properties and Gamma Radiation Shielding Capability of Transparent Barium Borosilicate Glass Composite. Sustainability 2022, 14, 13298.
11. Zhang, L.; Li, M.; Lyu, Q.; Zhu, J. Bioinspired Structural Color Nanocomposites with Healable Capability. Polym. Chem. 2020, 11, 6413–6422.
12. Forouzandeh, P.; Pillai, S.C. Two-Dimensional (2D) Electrode Materials for Supercapacitors. Mater. Today Proc. 2021, 41, 498–505.
13. Kim, S.; Lee, Y.M. Two-Dimensional Nanosheets and Membranes for Their Emerging Technologies. Curr. Opin. Chem. Eng. 2023, 39, 100893.
14. Tyagi, D.; Wang, H.; Huang, W.; Hu, L.; Tang, Y.; Guo, Z.; Ouyang, Z.; Zhang, H. Recent Advances in Two-Dimensional-Material- Based Sensing Technology toward Health and Environmental Monitoring Applications. Nanoscale 2020, 12, 3535–3559.
15. Chen, Y.; Zhao, X.; Li, Y.; Jin, Z.-Y.; Yang, Y.; Yang, M.-B.; Yin, B. Light-and Magnetic-Responsive Synergy Controlled Reconfiguration of Polymer Nanocomposites with Shape Memory Assisted Self-Healing Performance for Soft Robotics. J. Mater. Chem. C 2021, 9, 5515–5527.
16. Salahdin, O.D.; Sayadi, H.; Solanki, R.; Parra, R.M.R.; Al-Thamir, M.; Jalil, A.T.; Izzat, S.E.; Hammid, A.T.; Arenas, L.A.B.; Kianfar, E. Graphene and Carbon Structures and Nanomaterials for Energy Storage. Appl. Phys. A 2022, 128, 703.
17. Dong, Q.; Ryu, H.; Lei, Y. Metal Oxide Based Non-Enzymatic Electrochemical Sensors for Glucose Detection. Electrochim. Acta 2021, 370, 137744.
18. Li, C.; Wu, H.; Hong, S.; Wang, Y.; Song, N.; Han, Z.; Dong, H. 0D/2D Heterojunction Constructed by High-Dispersity Mo-Doped Ni2P Nanodots Supported on g-C3N4 Nanosheets towards Enhanced Photocatalytic H2 Evolution Activity. Int. J. Hydrogen Energy 2020, 45, 22556–22566.
19. Jin, X.; Gu, T.-H.; Lee, K.-G.; Kim, M.J.; Islam, M.S.; Hwang, S.-J. Unique Advantages of 2D Inorganic Nanosheets in Exploring High-Performance Electrocatalysts: Synthesis, Application, and Perspective. Coord. Chem. Rev. 2020, 415, 213280.
20. Zhang, C.; Chen, M.; Pan, Y.; Li, Y.; Wang, K.; Yuan, J.; Sun, Y.; Zhang, Q. Carbon Nanodots Memristor: An Emerging Candidate toward Artificial Biosynapse and Human Sensory Perception System. Adv. Sci. 2023, 10, 2207229.
21. Rasal, A.S.; Yadav, S.; Yadav, A.; Kashale, A.A.; Manjunatha, S.T.; Altaee, A.; Chang, J.-Y. Carbon Quantum Dots for Energy Applications: A Review. ACS Appl. Nano Mater. 2021, 4, 6515–6541.

22. Baruah, B.; Kumar, A. Platinum-Free Anode Electrocatalysts for Methanol Oxidation in Direct Methanol Fuel Cells. In Ceramic and Specialty Electrolytes for Energy Storage Devices; CRC Press: Boca Raton, FL, USA, 2021; pp. 261–283. ISBN 1003144810.
23. Niu, H.; Xia, C.; Huang, L.; Zaman, S.; Maiyalagan, T.; Guo, W.; You, B.; Xia, B.Y. Rational Design and Synthesis of One-Dimensional Platinum-Based Nanostructures for Oxygen-Reduction Electrocatalysis. Chin. J. Catal. 2022, 43, 1459–1472.
24. Mei, J.; Liao, T.; Ayoko, G.A.; Bell, J.; Sun, Z. Cobalt Oxide-Based Nanoarchitectures for Electrochemical Energy Applications. Prog. Mater. Sci. 2019, 103, 596–677.
25. Ganiyu, S.O.; Martínez-Huitle, C.A.; Rodrigo, M.A. Renewable Energies Driven ElectrochemicalWastewater/Soil Decontamination Technologies: A Critical Review of Fundamental Concepts and Applications. Appl. Catal. B Environ. 2020, 270, 118857.
26. Parveen, N.; Ansari, M.O.; Ansari, S.A.; Kumar, P. Nanostructured Titanium Nitride and Its Composites as High-Performance Supercapacitor Electrode Material. Nanomaterials 2022, 13, 105.
27. Zheng, S.; Zhang, J.; Deng, H.; Du, Y.; Shi, X. Chitin Derived Nitrogen-Doped Porous Carbons with Ultrahigh Specific Surface Area and Tailored Hierarchical Porosity for High Performance Supercapacitors. J. Bioresour. Bioprod. 2021, 6, 142–151.
28. Yadav, G.; Ahmaruzzaman, M. Recent Progress on Synthesis and Modifications of ZnIn2S4 Based Novel Hybrid Materials for Potential Applications. Mater. Sci. Eng. B 2023, 292, 116418.
29. Parveen, N.; Ansari, M.O.; Ansari, S.A.; Kumar, P. Nanostructured Titanium Nitride and Its Composites as High-Performance Supercapacitor Electrode Material. Nanomaterials 2022, 13, 105.
30. Yan, B.; Feng, L.; Zheng, J.; Zhang, Q.; Zhang, C.; Ding, Y.; Han, J.; Jiang, S.; He, S. In Situ Growth of N/O-Codoped Carbon Nanotubes inWood-Derived Thick Carbon Scaffold to Boost the Capacitive Performance. Colloids Surfaces A Physicochem. Eng. Asp. 2023, 662, 131018.
31. Yu, X.-Y.; Liu, Z.-G.; Huang, X.-J. Nanostructured Metal Oxides/Hydroxides-Based Electrochemical Sensor for Monitoring Environmental Micropollutants. Trends Environ. Anal. Chem. 2014, 3, 28–35.
32. Obodo, R.M.; Shinde, N.M.; Chime, U.K.; Ezugwu, S.; Nwanya, A.C.; Ahmad, I.; Maaza, M.; Ejikeme, P.M.; Ezema, F.I. Recent Advances in Metal Oxide/Hydroxide on Three-Dimensional Nickel Foam Substrate for High Performance Pseudocapacitive Electrodes. Curr. Opin. Electrochem. 2020, 21, 242–249.
33. Yang, T.; Xu, C.; Liu, C.; Ye, Y.; Sun, Z.; Wang, B.; Luo, Z. Conductive Polymer Hydrogels Crosslinked by Electrostatic Interaction with PEDOT: PSS Dopant for Bioelectronics Application. Chem. Eng. J. 2022, 429, 132430.
34. Yin, P.T.; Shah, S.; Chhowalla, M.; Lee, K.-B. Design, Synthesis, and Characterization of Graphene–Nanoparticle Hybrid Materials for Bioapplications. Chem. Rev. 2015, 115, 2483–2531.
35. Li, B.L.; Setyawati, M.I.; Zou, H.L.; Dong, J.X.; Luo, H.Q.; Li, N.B.; Leong, D.T. Emerging 0D Transition-metal Dichalcogenides for Sensors, Biomedicine, and Clean Energy. Small 2017, 13, 1700527.
36. Rajesh, D.; Francis, M.K.; Bhargav, P.B.; Nafis, A.; Balaji, C. 2D Layered Nickel-Cobalt Double Hydroxide Nano Sheets@ 1D Silver Nanowire-Graphitic Carbon Nitrides for High Performance Super Capacitors. J. Alloys Compd. 2022, 898, 162803.
37. Wirunchit, S.; Koetniyom,W. ZnO nanoparticles synthesis and characterization by hydrothermal process for biological applications. Physica Status Solidi (A) 2023, 220, 2200364.
38. Misra, K.P.; Jain, S.; Agarwala, A.; Halder, N.; Chattopadhyay, S. Effective mass model supported band gap variation in cobalt-doped ZnO nanoparticles obtained by co-precipitation. Semiconductors 2020, 54, 311–316.
39. Lin, K.F.; Cheng, H.M.; Hsu, H.C.; Lin, L.J.; Hsieh, W.F. Band gap variation of size-controlled ZnO quantum dots synthesized by sol–gel method. Chem. Phys. Lett. 2005, 409, 208–211.
40. Pecharsky, V.K.; Zavalij, P.Y. The powder diffraction pattern. In Fundamentals of Powder Diffraction and Structural Characterization of Materials; Springer: New York, NY, USA, 2009; pp. 151–202.
41. Bindu, P.; Thomas, S. Estimation of lattice strain in ZnO nanoparticles: X-ray peak profile analysis. J. Theor. Appl. Phys. 2014, 8, 123–134.